

Weak-light ultraslow vector solitons via electromagnetically induced transparency

Chao Hang

Institute of Theoretical Physics and Department of Physics, East China Normal University, Shanghai 200062, China

Guoxiang Huang*

State Key Laboratory of Precision Spectroscopy and Department of Physics, East China Normal University, Shanghai 200062, China

(Received 7 March 2007; revised manuscript received 29 November 2007; published 14 March 2008)

We propose a scheme to generate temporal vector optical solitons in a lifetime broadened five-state atomic medium via electromagnetically induced transparency. We show that this scheme, which is fundamentally different from the passive one by using optical fibers, is capable of achieving distortion-free vector optical solitons with ultraslow propagating velocity under very weak drive conditions. We demonstrate both analytically and numerically that it is easy to realize Manakov temporal vector solitons by actively manipulating the dispersion and self- and cross-phase modulation effects of the system.

DOI: [10.1103/PhysRevA.77.033830](https://doi.org/10.1103/PhysRevA.77.033830)

PACS number(s): 42.65.Tg, 42.50.Gy

I. INTRODUCTION

The vector nature of light propagating in a nonlinear medium has led to the discovery of a class of solitons, i.e., vector optical solitons, which are the solutions of two coupled nonlinear Schrödinger (NLS) equations describing the envelope evolution of two polarization components of an electromagnetic field. In recent years, considerable attention has been paid to the temporal [1–8] and spatial [9–13] vector optical solitons in various nonlinear systems. Due to their remarkable property, vector optical solitons have promising applications for the design of new types of all-optical switches and logic gates [14].

Up to now, most vector optical solitons are produced in passive media such as optical fibers [4–14], in which far-off resonance excitation schemes are employed in order to avoid unmanageable optical attenuation and distortion. However, due to the lack of distinctive energy levels, the nonlinear effect in such passive media is very weak. Consequently, to form vector solitons very high input light power and extended propagation distance are required. The propagating velocity of the vector solitons produced in passive media is also very close to c , the speed of light in vacuum. On the other hand, the lack of distinctive energy levels and transition selection rules also makes an active control very difficult. In particular, it is hard to realize Manakov [15] temporal vector optical solitons in optical fibers because the ratio between self-phase modulation (SPM) and cross-phase modulation (CPM) is not unity and there is also detrimental energy exchange between two polarization components due to the existence of the four-wave mixing effect. Manakov vector optical solitons are of great interest, not only because the coupled NLS equations describing them have interesting mathematical properties but also such solitons may have promising practical applications, e.g., for realizing all-optical computing [16]. Different from spatial Manakov vector optical solitons, which have been observed more than 10 years ago [11], temporal Manakov vector optical solitons have not been realized in experiment up to now.

It is well known that nonlinear optical processes can be largely enhanced by utilizing resonant atomic systems [17]. Unfortunately, attempts to use resonance enhancement have long been frustrated for many years by the problem associated with serious optical absorption. However, this paradigm has been challenged by the theoretical and experimental studies on electromagnetically induced transparency (EIT) [18], which has received considerable interest in recent years. For a three-state atomic system under EIT condition, the absorption of a probe laser field tuned to a strong one-photon resonance can be largely suppressed by the quantum interference effect induced by a coupling laser field, and hence an initially highly opaque optical medium may become transparent. The optical wave propagation in such system possesses many striking physical features, including the significant reduction of group velocity [19,20] and the tremendous enhancement of Kerr nonlinearity of the probe field [21,22]. Recently, the resonant EIT media have been used to realize the polarization qubit phase gate [23] and reversible memory devices for the photon-polarization qubit [24].

In this work, we propose an EIT scheme to generate temporal vector optical solitons in a resonant five-level atomic system. We show that two continuous-wave (cw) control fields established prior to the injection of a pulsed probe field induce a quantum interference effect, which can suppress largely the absorption of the two orthogonal polarization components of the probe field. The scheme suggested here is fundamentally different from the passive ones due to the existence of distinctive energy levels that make an active manipulation on the dispersion and nonlinear effects of the system possible. In addition, contrary to all passive schemes the vector optical solitons produced in the present system may have ultraslow propagating velocity and their production needs only very weak input power and very short propagating distance. Furthermore, the controllability of the present scheme allows us also to realize easily temporal Manakov vector optical solitons by actively adjusting the parameters of the system. Notice that scalar ultraslow optical solitons and soliton pairs in EIT media have been investigated recently [25–29]. The formation of the weak-light scalar spatial solitons and the two-component Thirring-type spatial solitons have also been investigated in EIT-based systems

*Corresponding author. gxhuang@phy.ecnu.edu.cn

[30–33]. However, up to now there has been no study on the ultraslow vector optical solitons in an active optical medium. Our study represents an achievement in this direction and the results may have potential application in optical information processing and engineering.

The paper is arranged as follows. In the next section, the theoretical model under study is introduced and its solution in linear regime is presented. In Sec. III, an asymptotic expansion on the Maxwell-Schrödinger equations is made and the coupled NLS equations governing the time evolution of two polarization components of the probe field are derived by means of a method of multiple scales. In Sec. IV, weak-light ultraslow vector soliton solutions are provided and their stability and controllability during propagation are discussed in detail. In addition, the collisions between two ultraslow vector solitons are also investigated numerically. Finally, the last section contains a discussion and summary of the main results of our work.

II. MODEL AND SOLUTION IN LINEAR REGIME

Consider a lifetime broadened five-level system (e.g., a Zeeman split atomic gas) interacting with a weak, linear-polarized pulsed probe field of central frequency and two strong, linear-polarized cw control fields of frequencies $\omega_{c1}/(2\pi)$ and $\omega_{c2}/(2\pi)$, respectively. The two polarization components of the probe field drive, respectively, the transitions from $|3\rangle \leftrightarrow |2\rangle$ and $|3\rangle \leftrightarrow |4\rangle$, while the two control fields drive, respectively, the transitions from $|1\rangle \leftrightarrow |2\rangle$ and $|5\rangle \leftrightarrow |4\rangle$ [see Fig. 1(a)]. The atoms are trapped in a cell at enough low temperature to cancel Doppler broadening and reduce interatomic collisions. A possible arrangement of experimental apparatus is shown in Fig. 1(b).

The electric field of the system can be written as $\mathbf{E} = (\hat{\mathbf{e}}_+ \mathcal{E}_{p+} + \hat{\mathbf{e}}_- \mathcal{E}_{p-}) \exp[i(k_p z - \omega_p t)] + \hat{\mathbf{e}}_{c1} \mathcal{E}_{c1} \exp[i(\mathbf{k}_{c1} \cdot \mathbf{r} - \omega_{c1} t)] + \hat{\mathbf{e}}_{c2} \mathcal{E}_{c2} \exp[i(\mathbf{k}_{c2} \cdot \mathbf{r} - \omega_{c2} t)] + \text{c.c.}$ Here $\hat{\mathbf{e}}_+ = (\hat{\mathbf{x}} + i\hat{\mathbf{y}})/\sqrt{2}$ [$\hat{\mathbf{e}}_- = (\hat{\mathbf{x}} - i\hat{\mathbf{y}})/\sqrt{2}$] is the probe-field unit vector of the σ^+ (σ^-) circular polarization component with the envelope \mathcal{E}_{p+} (\mathcal{E}_{p-}), which drives the transition $|3\rangle \leftrightarrow |4\rangle$ ($|2\rangle \leftrightarrow |3\rangle$). $\hat{\mathbf{e}}_{c1}$ ($\hat{\mathbf{e}}_{c2}$) is the unit vector of the control field with the envelope \mathcal{E}_{c1} (\mathcal{E}_{c2}), which drives the transition $|1\rangle \leftrightarrow |2\rangle$ ($|4\rangle \leftrightarrow |5\rangle$). Thus the system is composed of two EIT Λ configurations, both of them share the ground-state level $|3\rangle$ [23,24].

The Hamiltonian of the system has the form $\hat{H} = \hat{H}_0 + \hat{H}'$, where \hat{H}_0 describes a free atom and \hat{H}' describes the interaction between the atom and the optical field. In the Schrödinger picture, the state vector of the systems is expressed by $|\Psi(t)\rangle_s = \sum_{j=1}^5 C_j(z, t) |j\rangle$, where $|j\rangle$ is the eigenstate of \hat{H}_0 . Under electric-dipole and rotating-wave approximations, the Hamiltonian of the system takes the form

$$\begin{aligned} \hat{H} = & \sum_{j=1}^5 \epsilon_j |j\rangle \langle j| + \hbar \{ \Omega_{c1} \exp[i(\mathbf{k}_{c1} \cdot \mathbf{r} - \omega_{c1} t)] |2\rangle \langle 1| \\ & + \Omega_{p1} \exp[i(k_p z - \omega_p t)] |2\rangle \langle 3| \\ & + \Omega_{p2} \exp[i(k_p z - \omega_p t)] |4\rangle \langle 3| \\ & + \Omega_{c2} \exp[i(\mathbf{k}_{c2} \cdot \mathbf{r} - \omega_{c2} t)] |4\rangle \langle 5| + \text{H.c.} \}, \end{aligned} \quad (1)$$

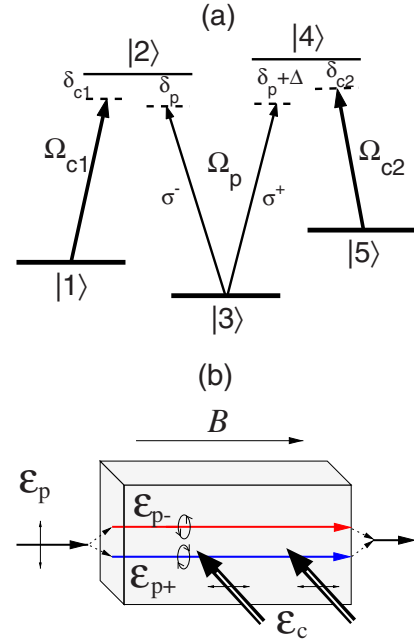


FIG. 1. (Color online) (a) Energy levels and excitation scheme of the lifetime broadened five-level atomic system. Ω_p is the Rabi frequency of the weak probe field with the σ_- (σ_+) component coupling to the energy levels $|3\rangle$ and $|2\rangle$ ($|3\rangle$ and $|4\rangle$). Ω_{c1} (Ω_{c2}) is the Rabi frequency of strong cw control field coupling to the energy levels $|1\rangle$ and $|2\rangle$ ($|5\rangle$ and $|4\rangle$). δ_{cl} ($l=1,2$) and δ_p are detunings, $\Delta = (2\mu_B/\hbar)gB$ with B the applied magnetic field. (b) Possible arrangement of experimental apparatus. \mathcal{E}_c represents the control field and \mathcal{E}_{p+} (\mathcal{E}_{p-}) represents the σ_- (σ_+) component of the probe field, respectively.

where ϵ_j is the energy of state $|j\rangle$, $\Omega_{p1} = -(\mathbf{p}_{23} \cdot \hat{\mathbf{e}}_-) \mathcal{E}_{p-} / \hbar$, $\Omega_{p2} = -(\mathbf{p}_{43} \cdot \hat{\mathbf{e}}_+) \mathcal{E}_{p+} / \hbar$, $\Omega_{c1} = -(\mathbf{p}_{21} \cdot \hat{\mathbf{e}}_{c1}) \mathcal{E}_{c1} / \hbar$, and $\Omega_{c2} = -(\mathbf{p}_{45} \cdot \hat{\mathbf{e}}_{c2}) \mathcal{E}_{c2} / \hbar$ are one-half Rabi frequencies with \mathbf{p}_{ij} being the electric-dipole matrix element associated with the transition from $|j\rangle$ and $|i\rangle$.

In order to investigate the dynamics of the system, it is more convenient to employ an interaction picture to eliminate the fast dependence on the spatial-temporal variables, which is obtained by making the transformation $C_j = A_j \exp[i(\mathbf{k}_j \cdot \mathbf{r} - (\epsilon_j/\hbar + \lambda_j)t)]$, with $\mathbf{k}_1 = k_p \mathbf{e}_z - \mathbf{k}_{c1}$, $\mathbf{k}_2 = k_p \mathbf{e}_z$, $\mathbf{k}_3 = 0$, $\mathbf{k}_5 = k_p \mathbf{e}_z - \mathbf{k}_{c2}$, $\lambda_1 = \delta_p - \delta_{c1}$, $\lambda_2 = \delta_p$, $\lambda_3 = 0$, $\lambda_4 = \delta_p + \Delta$, and $\lambda_5 = \delta_p + \Delta - \delta_{c2}$. The detunings are defined as $\delta_p = (\epsilon_2 - \epsilon_3)/\hbar - \omega_p$, $\delta_{c1} = (\epsilon_2 - \epsilon_1)/\hbar - \omega_{c1}$, and $\delta_{c2} = (\epsilon_4 - \epsilon_5)/\hbar - \omega_{c2}$. $\Delta = (2\mu_B/\hbar)gB$ is the Zeeman shift of the upper atomic sublevel with μ_B the Bohr magneton, g the gyromagnetic factor, and B the applied magnetic field. Then under electric-dipole and rotating-wave approximations we obtain the Hamiltonian in the interaction picture

$$\begin{aligned} \hat{H}_{\text{int}} = & \hbar [(\delta_p - \delta_{c1}) |1\rangle \langle 1| + \delta_p |2\rangle \langle 2| \\ & + (\delta_p + \Delta) |4\rangle \langle 4| + (\delta_p + \Delta - \delta_{c2}) |5\rangle \langle 5|] \\ & + \hbar [\Omega_{c1} |2\rangle \langle 1| + \Omega_{p1} |2\rangle \langle 3| \\ & + \Omega_{p2} |4\rangle \langle 3| + \Omega_{c2} |4\rangle \langle 5| + \text{H.c.}], \end{aligned} \quad (2)$$

Using the Schrödinger equation $i\hbar \partial |\Psi(t)\rangle_{\text{int}} / \partial t = H_{\text{int}} |\Psi(t)\rangle_{\text{int}}$ with $|\Psi(t)\rangle_{\text{int}} = (A_1, A_2, A_3, A_4, A_5)^T$ (T represents transpose) one can readily obtain the equations governing the atomic response of the system,

$$\left(\frac{\partial}{\partial t} + id_1\right)A_1 = -i\Omega_{c1}^* A_2, \quad (3a)$$

$$\left(\frac{\partial}{\partial t} + id_2\right)A_2 = -i\Omega_{c1} A_1 - i\Omega_{p1} A_3, \quad (3b)$$

$$\left(\frac{\partial}{\partial t} + id_4\right)A_4 = -i\Omega_{c2} A_5 - i\Omega_{p2} A_3, \quad (3c)$$

$$\left(\frac{\partial}{\partial t} + id_5\right)A_5 = -i\Omega_{c2}^* A_4, \quad (3d)$$

with $\sum_{j=1}^5 |A_j|^2 = 1$. In Eqs. (3a)–(3d) we have defined $d_1 = (\delta_p - \delta_{c1}) - i\Gamma_1/2$, $d_2 = \delta_p - i\Gamma_2/2$, $d_3 = -i\Gamma_3/2$, $d_4 = (\delta_p + \Delta) - i\Gamma_4/2$, and $d_5 = (\delta_p + \Delta - \delta_{c2}) - i\Gamma_5/2$ with Γ_j .

To obtain the equations of motion for $\Omega_{p1}(z, t)$ and $\Omega_{p2}(z, t)$, we use the Maxwell equation

$$\nabla^2 \mathbf{E} - \frac{1}{c^2} \frac{\partial^2 \mathbf{E}}{\partial t^2} = \frac{1}{\epsilon_0 c^2} \frac{\partial^2 \mathbf{P}}{\partial t^2} \quad (4)$$

with

$$\begin{aligned} \mathbf{P} = & \mathcal{N}_a \{ \mathbf{p}_{21} A_2 A_1^* \exp[i(\mathbf{k}_{c1} \cdot \mathbf{r} - \omega_{c1} t)] \\ & + \mathbf{p}_{23} A_2 A_3^* \exp[i(k_p z - \omega_p t)] \\ & + \mathbf{p}_{43} A_4 A_3^* \exp[i(k_p z - \omega_p t)] \\ & + \mathbf{p}_{45} A_4 A_5^* \exp[i(\mathbf{k}_{c2} \cdot \mathbf{r} - \omega_{c2} t)] + \text{c.c.} \}. \end{aligned}$$

Under slowly varying envelope approximation, Eq. (4) is reduced to

$$i \left(\frac{\partial}{\partial z} + \frac{1}{c} \frac{\partial}{\partial t} \right) \Omega_{p1} - \kappa_{32} A_2 A_3^* = 0, \quad (5a)$$

$$i \left(\frac{\partial}{\partial z} + \frac{1}{c} \frac{\partial}{\partial t} \right) \Omega_{p2} - \kappa_{34} A_4 A_3^* = 0; \quad (5b)$$

in Eqs. (5a) and (5b), $\kappa_{32} = \mathcal{N}_a |\mathbf{p}_{32} \cdot \hat{\epsilon}_-|^2 \omega_p / (2\hbar \epsilon_0 c)$ and $\kappa_{34} = \mathcal{N}_a |\mathbf{p}_{34} \cdot \hat{\epsilon}_+|^2 \omega_p / (2\hbar \epsilon_0 c)$, with \mathcal{N}_a being the atomic density, ϵ_0 the vacuum dielectric constant.

Before solving the nonlinearly coupled equations (3a)–(3d), (5a), and (5b), let us first examine the linear excitations of the system, which may provide useful hints of the weak nonlinear theory developed in the next section. Assuming Ω_{p1} , Ω_{p2} , and A_j ($j=1, 2, 4, 5$) are small and proportional to $\exp[i[k(\omega)z - \omega t]$ so that the atomic ground state $|3\rangle$ is not depleted (i.e., $A_3=1$), one can obtain two branches of linear dispersion relation for the linear excitations,

$$k_1(\omega) = \frac{\omega}{c} + \kappa_{32} \frac{\omega - d_1}{D_1(\omega)}, \quad (6)$$

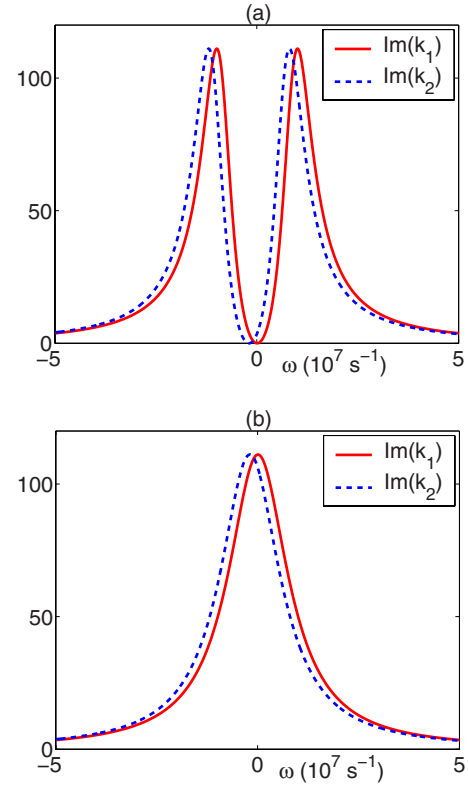


FIG. 2. (Color online) Absorption spectra $\text{Im}[k_1(\omega)]$ (solid line) and $\text{Im}[k_2(\omega)]$ (dashed line) for the probe field component Ω_{p1} and Ω_{p2} . (a) EIT case ($\Omega_{c1} = \Omega_{c2} = 1.0 \times 10^7 \text{ s}^{-1}$). (b) Non-EIT case ($\Omega_{c1} = \Omega_{c2} = 0$).

$$k_2(\omega) = \frac{\omega}{c} + \kappa_{34} \frac{\omega - d_5}{D_2(\omega)}, \quad (7)$$

corresponding to σ^- and σ^+ components of the probe field, respectively. In Eqs. (6) and (7) we have defined $D_1(\omega) = |\Omega_{c1}|^2 - (\omega - d_1)(\omega - d_2)$ and $D_2(\omega) = |\Omega_{c2}|^2 - (\omega - d_4)(\omega - d_5)$.

Shown in Fig. 2(a) is the absorption spectra of Ω_{p1} (solid line) and Ω_{p2} (dashed line) when taking $\Omega_{c1} = \Omega_{c2} = 1.0 \times 10^7 \text{ s}^{-1}$ (EIT case). The other parameters are chosen as $\Gamma_2 = \Gamma_4 = \Gamma = 2\pi \times 6.0 \text{ MHz}$, $\Gamma_1 = \Gamma_3 = \Gamma_5 = 10^{-4} \Gamma$, $\kappa_{32} \approx \kappa_{34} = 1.0 \times 10^9 \text{ cm}^{-1} \text{ s}^{-1}$, $\delta_p = \delta_{c1} = \delta_{c2} = 0$, and $\Delta = 2.0 \times 10^6 \text{ s}^{-1}$. We see that due to the contribution of the control fields Autler-Townes doublets open for both absorption spectra. In addition, near the central frequency of the probe field (i.e., $\omega=0$) one has $\text{Im}(k_1) \approx 0$ and $\text{Im}(k_2) \approx 0$, i.e., the absorption of the probe field is almost completely suppressed. In contrast, when the control fields are switched off, i.e., $\Omega_{c1} = \Omega_{c2} = 0$ (non-EIT case), the absorption of the probe field is maximum near $\omega=0$, as shown in Fig. 2(b). The physical reason of the suppression of the probe-field absorption shown in the EIT case [Fig. 2(a)] is that the two strong control fields induce a quantum destructive interference effect, which make the population in the levels $|2\rangle$ and $|4\rangle$ vanish and hence the two polarization components of the probe field become transparent in this five-level resonant system.

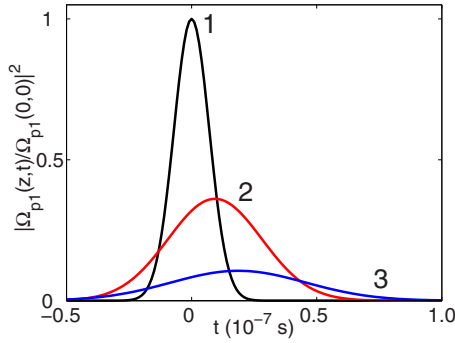


FIG. 3. (Color online) The dimensionless probe wave intensity $|\Omega_{p1}(z,t)/\Omega_{p1}(0,0)|^2$ when propagating to the distance $z=0.1$ cm (curve 2) and 0.2 cm (curve 3), respectively. The initial condition is a Gaussian pulse with the form $\Omega_{p1}(0,t)=\Omega_{p1}(0,0)\exp[-t^2/(2\tau_0^2)]$ (curve 1), with $\tau_0=1.0\times 10^{-8}$ s and other parameters being the same as those used in Fig. 2.

Although the absorption of the system can be largely suppressed by the introduction of the control fields, the dispersion effect may be significant for the probe pulse with a shorter temporal width. Figure 3 shows the dimensionless probe field intensity $|\Omega_{p1}(z,t)/\Omega_{p1}(0,0)|^2$ when propagating to the distance $z=0.1$ cm (curve 2) and 0.2 cm (curve 3). A similar plot for $|\Omega_{p2}(z,t)/\Omega_{p2}(0,0)|^2$ can also be obtained. The initial condition is a Gaussian pulse with the form $\Omega_{p1}(0,t)=\Omega_{p1}(0,0)\exp[-t^2/(2\tau_0^2)]$ (curve 1), with $\tau_0=1.0\times 10^{-8}$ s and other parameters being the same as those used in Fig. 2. We see that due to the dispersion effect of the system, the probe pulse spreads rapidly. The main contribution for the pulse spread is mainly due to the group-velocity dispersion of the system.

III. ASYMPTOTIC EXPANSION AND COUPLED NLS EQUATIONS

We are interested in a shape-preserving propagation of the probe pulse, which is desirable for the applications of optical information processing and transmission. As shown in the last section, the dispersion effect of the system makes the probe pulse broaden and hence one should find a way to stop the dispersion to obtain a stable pulse propagation in the system. In the following we show that if using a probe pulse with larger intensity, the self-phase modulation and cross-phase modulation effects of the two components of the probe field can balance the group-velocity dispersion and form weak-light ultraslow vector solitons in the system.

To this aim, we apply the standard method of multiple scales [34] to investigate the weak nonlinear evolution of the probe field. We make the asymptotic expansion $A_j = \sum_{l=0}^{\infty} \mu^l A_j^{(l)}$, $\Omega_{p1} = \sum_{l=1}^{\infty} \mu^l \Omega_{p1}^{(l)}$, and $\Omega_{p2} = \sum_{l=1}^{\infty} \mu^l \Omega_{p2}^{(l)}$ with $A_3^{(0)} = 1$ and $A_j^{(0)} = 0$ ($j=1,2,4,5$), where μ is a small parameter characterizing the small population depletion of the ground state and all quantities on the right-hand side of the asymptotic expansion are considered as functions of the multiscale variables $z_l = \mu^l z$ ($l=0,1,2$) and $t_l = \mu^l t$ ($l=0,1$). Substituting such expansion into Eqs. (3a)–(3d) and (4), we obtain

$$\left(\frac{\partial}{\partial t_0} + id_1\right)A_1^{(l)} + i\Omega_{c1}^* A_2^{(l)} = M^{(l)}, \quad (8a)$$

$$\left(\frac{\partial}{\partial t_0} + id_2\right)A_2^{(l)} + i\Omega_{c1} A_1^{(l)} + i\Omega_{p1}^{(l)} = N^{(l)}, \quad (8b)$$

$$\left(\frac{\partial}{\partial t_0} + id_4\right)A_4^{(l)} + i\Omega_{c2} A_5^{(l)} + i\Omega_{p2}^{(l)} = P^{(l)}, \quad (8c)$$

$$\left(\frac{\partial}{\partial t_0} + id_5\right)A_5^{(l)} + i\Omega_{c2}^* A_4^{(l)} = Q^{(l)}, \quad (8d)$$

and

$$i\left(\frac{\partial}{\partial z_0} + \frac{1}{c} \frac{\partial}{\partial t_0}\right)\Omega_{p1}^{(l)} - \kappa_{32} A_2^{(l)} = R^{(l)}, \quad (9a)$$

$$i\left(\frac{\partial}{\partial z_0} + \frac{1}{c} \frac{\partial}{\partial t_0}\right)\Omega_{p2}^{(l)} - \kappa_{34} A_4^{(l)} = T^{(l)}, \quad (9b)$$

where the quantities $M^{(l)}$, $N^{(l)}$, $P^{(l)}$, $Q^{(l)}$, $R^{(l)}$, and $T^{(l)}$ on the right-hand side of the above equations have been given in the Appendix.

It is convenient to express Eqs. (8a)–(8d), (9a), and (9b) in the following forms:

$$\hat{\mathcal{L}}_1 \Omega_{p1}^{(l)} = S_1^{(l)}, \quad (10a)$$

$$\hat{\mathcal{L}}_2 \Omega_{p2}^{(l)} = S_2^{(l)}, \quad (10b)$$

$$A_1^{(l)} = \frac{1}{i\Omega_{c1}} \left[N^{(l)} - \left(\frac{\partial}{\partial t_0} + id_2\right)A_2^{(l)} - i\Omega_{p1}^{(l)} \right], \quad (10c)$$

$$A_2^{(l)} = -\frac{1}{\kappa_{32}} \left[R^{(l)} - i\left(\frac{\partial}{\partial z_0} + \frac{1}{c} \frac{\partial}{\partial t_0}\right)\Omega_{p1}^{(l)} \right], \quad (10d)$$

$$A_4^{(l)} = -\frac{1}{\kappa_{34}} \left[T^{(l)} - i\left(\frac{\partial}{\partial z_0} + \frac{1}{c} \frac{\partial}{\partial t_0}\right)\Omega_{p2}^{(l)} \right], \quad (10e)$$

$$A_5^{(l)} = \frac{1}{i\Omega_{c2}} \left[P^{(l)} - \left(\frac{\partial}{\partial t_0} + id_4\right)A_4^{(l)} - i\Omega_{p2}^{(l)} \right], \quad (10f)$$

where the explicit expressions of the operators $\hat{\mathcal{L}}_1$, $\hat{\mathcal{L}}_2$ and the quantities $S_1^{(l)}$ and $S_2^{(l)}$ in Eqs. (10a) and (10b) have also been given in the Appendix.

It is easy to find the leading order ($l=1$) solution of Eqs. (10a) and (10b),

$$\Omega_{p1}^{(1)} = F_1 \exp\{i[k_1(\omega)z_0 - \omega t_0]\}, \quad (11a)$$

$$\Omega_{p2}^{(1)} = F_2 \exp\{i[k_2(\omega)z_0 - \omega t_0]\}, \quad (11b)$$

where $F_{1,2}$ are yet to be determined envelope functions of the slow variables t_1 , z_1 , and z_2 . The expressions of $A_j^{(1)}$ ($j=1,2,4,5$) can also be obtained readily by using Eqs. (10c)–(10f), which are omitted here.

At the second order ($l=2$), the solvability conditions for obtaining divergence-free solution for $\Omega_{p1}^{(2)}$ and $\Omega_{p2}^{(2)}$ requires

$$i\left(\frac{\partial F_1}{\partial t_1} + V_{g1} \frac{\partial F_1}{\partial z_1}\right) = 0, \quad (12a)$$

$$i\left(\frac{\partial F_2}{\partial t_1} + V_{g2} \frac{\partial F_2}{\partial z_1}\right) = 0, \quad (12b)$$

with $V_{g1}=1/K_{11}$ and $V_{g2}=1/K_{21}$, where $K_{11}=1/c + \kappa_{32}(|\Omega_{c1}|^2 + d_1^2)/(|\Omega_{c1}|^2 - d_1 d_2)^2$ and $K_{21}=1/c + \kappa_{34}(|\Omega_{c2}|^2 + d_5^2)/(|\Omega_{c2}|^2 - d_4 d_5)^2$ are the group velocities of the σ^- and σ^+ components of the probe field.

With the above results we go to the third order ($l=3$). The solvability conditions in this order yields the coupled NLS equations governing the spatial-temporal evolution of $F_{1,2}$,

$$i\frac{\partial F_1}{\partial z_2} - \frac{K_{12}}{2} \frac{\partial^2 F_1}{\partial t_1^2} - (W_{11}|F_1|^2 + W_{12}|F_2|^2)e^{-2\bar{\alpha}_{1z_2}} F_1 = 0, \quad (13a)$$

$$i\frac{\partial F_2}{\partial z_2} - \frac{K_{22}}{2} \frac{\partial^2 F_2}{\partial t_1^2} - (W_{21}|F_1|^2 + W_{22}|F_2|^2)e^{-2\bar{\alpha}_{2z_2}} F_2 = 0, \quad (13b)$$

where

$$K_{12,22} = -2\kappa_{32,34} \frac{d_{2,4}|\Omega_{c1,c2}|^2 + 2d_{1,5}|\Omega_{c1,c2}|^2 + d_{1,5}^3}{(|\Omega_{c1,c2}|^2 - d_{2,4}d_{1,5})^3}, \quad (14)$$

$$W_{11,22} = -\kappa_{32,34} \frac{d_{1,5}(|d_{1,5}|^2 + |\Omega_{c1,c2}|^2)}{D_{1,2}|D_{1,2}|^2}, \quad (15)$$

$$W_{12,21} = -\kappa_{32,34} \frac{d_{1,5}(|d_{5,1}|^2 + |\Omega_{c2,c1}|^2)}{D_{1,2}|D_{2,1}|^2}. \quad (16)$$

In Eqs. (12a), (12b), (13a), and (13b) we have defined $K_{1j} = [\partial^j k_1(\omega)/\partial \omega^j]_{\omega=0}$ and $K_{2j} = [\partial^j k_2(\omega)/\partial \omega^j]_{\omega=0}$ ($j=0, 1, 2, \dots$). The coefficients K_{12} and K_{22} characterize the group-velocity dispersion, W_{11} and W_{22} characterize the SPM, and W_{12} and W_{21} characterize the CPM of the σ^- and σ^+ components of the probe field, respectively, $\bar{\alpha}_{1,2} = \mu^2 \alpha_{1,2}$ with $\alpha_{1,2} = \text{Im}[K_{10,20}]$.

By introducing $\delta = (1/V_{g1} - 1/V_{g2})/2$, $V_g = 2V_{g1}V_{g2}/(V_{g1} + V_{g2})$, and $\tau = t - z/V_g$, Eqs. (13a) and (13b) can be written as the dimensionless form

$$i\left(\frac{\partial}{\partial s} + g_{A1}\right)u_1 + ig_\delta \frac{\partial u_1}{\partial \sigma} - \frac{g_{D1}}{2} \frac{\partial^2 u_1}{\partial \sigma^2} - (g_{11}|u_1|^2 + g_{12}|u_2|^2)u_1 = 0, \quad (17a)$$

$$i\left(\frac{\partial}{\partial s} + g_{A2}\right)u_2 - ig_\delta \frac{\partial u_2}{\partial \sigma} - \frac{g_{D2}}{2} \frac{\partial^2 u_2}{\partial \sigma^2} - (g_{22}|u_2|^2 + g_{21}|u_1|^2)u_2 = 0, \quad (17b)$$

after returning to the original variables, where $s = z/L_D$, $\sigma = \tau/\tau_0$, $u_l = (\Omega_{pl}/U_0)\exp(-i\tilde{K}_{l0}z)$, ($\tilde{K}_{l0} = \text{Re}[K_{l0}]$), $g_{Al} = \alpha_l L_D$ ($l=1, 2$), $g_\delta = \text{sgn}(\delta)L_D/L_\delta$, $g_{D1} = K_{12}/|K_{22}|$, $g_{D2} = \text{sgn}(K_{22})$, and $g_{lm} = W_{lm}/|W_{22}|$ ($l, m=1, 2$). In these expressions we have defined the characteristic dispersion length $L_D = \tau_0^2/|K_{22}|$, and the characteristic group velocity mismatch length $L_\delta = \tau_0/|\delta|$, with τ_0 being the characteristic pulse length of the probe field. Since our aim is to obtain soliton solutions, in Eqs. (17a) and (17b) we have assumed the characteristic dispersion length L_D is equal to the characteristic nonlinear length of the system, which is defined by $L_{NL} = 1/(U_0^2|W_{22}|)$.

IV. VECTOR SOLITON SOLUTIONS

Because of the highly resonant character of the system, the coefficients in the coupled NLS equations (17a) and (17b) are generally complex and hence a soliton solution does not exist. However, due to the EIT effect induced by the two cw control fields the imaginary parts of these complex coefficients can be much smaller than their corresponding real parts. This important property leads Eqs. (17a) and (17b) to be nearly integrable and hence shape-preserving vector optical soliton solutions are possible that can propagate for an extended distance without significant deformation in the system.

It is easy to obtain bright-bright, bright-dark, and dark-dark vector soliton solutions of Eqs. (17a) and (17b) when disregarding the small imaginary parts of the coefficients. The bright-bright vector soliton solution reads as

$$u_1 = \mathcal{V}_1 \text{sech}(A\sigma + Bs)\exp[i(\mathcal{P}_1\sigma + \mathcal{Q}_1s)], \quad (18a)$$

$$u_2 = \mathcal{V}_2 \text{sech}(A\sigma + Bs)\exp[i(\mathcal{P}_2\sigma + \mathcal{Q}_2s)], \quad (18b)$$

if the parameters fulfill the condition $g_{22}g_{D1} = g_{12}g_{D2}$. Here we have defined $\mathcal{P}_1 = (B + g_\delta A)/(g_{D1}A)$, $\mathcal{P}_2 = (B - g_\delta A)/(g_{D2}A)$, $\mathcal{Q}_1 = -\mathcal{P}_1 g_\delta - g_{D1}(A^2 - \mathcal{P}_1^2)/2$, $\mathcal{Q}_2 = \mathcal{P}_2 g_\delta - g_{D2}(A^2 - \mathcal{P}_2^2)/2$, and $\mathcal{V}_2 = [(g_{D1}A^2 - g_{11}\mathcal{V}_1^2)/g_{12}]^{1/2}$.

A bright-dark vector soliton solution is given by

$$u_1 = \mathcal{V}_1 \text{sech}(A\sigma + Bs)\exp[i(\mathcal{P}_1\sigma + \mathcal{Q}_1s)], \quad (19a)$$

$$u_2 = \mathcal{V}_2 \tanh(A\sigma + Bs)\exp[i(\mathcal{P}_2\sigma + \mathcal{Q}_2s)], \quad (19b)$$

where $\mathcal{P}_1 = (B + g_\delta A)/(g_{D1}A)$, $\mathcal{P}_2 = (B - g_\delta A)/(g_{D2}A)$, $\mathcal{Q}_1 = -\mathcal{P}_1 g_\delta - g_{D1}(A^2 - \mathcal{P}_1^2)/2 - g_{12}\mathcal{V}_2^2$, $\mathcal{Q}_2 = \mathcal{P}_2 g_\delta + g_{D2}\mathcal{P}_2^2/2 - g_{22}\mathcal{V}_2^2$, and $\mathcal{V}_2 = [(g_{11}\mathcal{V}_1^2 - g_{D1}A^2)/g_{12}]^{1/2}$.

One can also obtain the dark-dark vector soliton solution

$$u_1 = \mathcal{V}_1 \tanh(A\sigma + Bs)\exp[i(\mathcal{P}_1\sigma + \mathcal{Q}_1s)], \quad (20a)$$

$$u_2 = \mathcal{V}_2 \tanh(A\sigma + Bs)\exp[i(\mathcal{P}_2\sigma + \mathcal{Q}_2s)], \quad (20b)$$

where $\mathcal{P}_1 = (B + g_\delta A)/(g_{D1}A)$, $\mathcal{P}_2 = (B - g_\delta A)/(g_{D2}A)$, $\mathcal{Q}_1 = -\mathcal{P}_1 g_\delta + g_{D1}(2A^2 + \mathcal{P}_1^2)/2$, $\mathcal{Q}_2 = \mathcal{P}_2 g_\delta + g_{D2}(2A^2 + \mathcal{P}_2^2)/2$, and $\mathcal{V}_2 = [-(g_{11}\mathcal{V}_1^2 + g_{D1}A^2)/g_{12}]^{1/2}$. In Eqs. (18a), (18b), (19a), (19b), (20a), and (20b) A , B , and \mathcal{V}_1 are free parameters ($A \neq 0$).

The formation of the vector optical soliton solutions given above are due to the balance between the group-velocity dispersion and nonlinearity (i.e., SPM and CPM) effects. We stress that since the SPM and the CPM coefficients defined by Eqs. (15) and (16) satisfy the following relation,

$$W_{11}W_{22} = W_{12}W_{21}, \quad (21)$$

then all three types of vector soliton solutions listed in Eqs. (18a), (18b), (19a), (19b), (20a), and (20b) are allowed in our system. This is very different from conventional systems (such as optical fibers), where the system parameters allow usually only one type of vector soliton.

We now give a practical example to show that a realistic atomic system can be found that allows the bright-bright vector optical soliton described above. We consider a cold alkali atomic vapor with the decay rates $\Gamma_2 \approx \Gamma_4 = 0.5 \times 10^7 \text{ s}^{-1}$ and $\Gamma_1 \approx \Gamma_3 \approx \Gamma_5 = 1.0 \times 10^4 \text{ s}^{-1}$. We take $\kappa_{32} \approx \kappa_{34} = 1.0 \times 10^9 \text{ cm}^{-1} \text{ s}^{-1}$ ($N_a \sim 10^{10} \text{ cm}^{-3}$), $\Omega_{c1} = \Omega_{c2} = 1.6 \times 10^8 \text{ s}^{-1}$, $\delta_p = 1.0 \times 10^8 \text{ s}^{-1}$, $\Delta = 2.0 \times 10^6 \text{ s}^{-1}$, $\delta_{c1} = 0$, and $\delta_{c2} = 3.0 \times 10^6 \text{ s}^{-1}$. With the above parameters, we obtain $K_{10} = -6.41 + 0.10i \text{ cm}^{-1}$, $K_{20} = -6.38 + 0.10i \text{ cm}^{-1}$, $K_{11} = (14.62 - 0.47i) \times 10^{-8} \text{ cm}^{-1} \text{ s}$, $K_{21} = (14.72 - 0.47i) \times 10^{-8} \text{ cm}^{-1} \text{ s}$, $K_{12} = (-4.56 + 0.25i) \times 10^{-15} \text{ cm}^{-1} \text{ s}^2$, $K_{22} = (-4.64 + 0.26i) \times 10^{-15} \text{ cm}^{-1} \text{ s}^2$, $W_{11} = (-9.37 + 0.15i) \times 10^{-16} \text{ cm}^{-1} \text{ s}^2$, $W_{12} = (-9.44 + 0.15i) \times 10^{-16} \text{ cm}^{-1} \text{ s}^2$, $W_{21} = (-9.34 + 0.15i) \times 10^{-16} \text{ cm}^{-1} \text{ s}^2$, and $W_{22} = (-9.40 + 0.15i) \times 10^{-16} \text{ cm}^{-1} \text{ s}^2$. Notice that the imaginary parts of these quantities are indeed much smaller than their relevant real parts. As mentioned above the physical reason for such small imaginary parts is due to quantum interference effect induced by two cw control fields (i.e., EIT effect). We obtain $L_\delta = 116.8 \text{ cm}$ and $L_D = 0.8 \text{ cm}$ with $\tau_0 = 6.0 \times 10^{-8} \text{ s}$ and $U_0 = 3.7 \times 10^7 \text{ s}^{-1}$. The dimensionless coefficients read $g_\delta = 0.007$, $g_{D1} = -0.98$, $g_{D2} = -1.0$, and $g_{11} \approx g_{12} \approx g_{21} \approx g_{22} = -1.0$. The group velocities of the two polarization components are given by

$$\text{Re}(V_{g1}) = 2.28 \times 10^{-4} c, \quad (22)$$

$$\text{Re}(V_{g2}) = 2.26 \times 10^{-4} c, \quad (23)$$

respectively, which means that the two polarization components of the vector optical soliton propagate with nearly matched, ultraslow propagating velocities comparing with c .

As we have emphasized, different from the passive media such as optical fibers [4–9, 11–13] the parameters of our present EIT medium can be actively manipulated. Consequently, the coefficients of Eqs. (17a) and (17b) can be easily adjusted to allow us to realize a temporal Manakov system, which is a completely integrable and can be solved by inverse-scattering transform [15]. In fact, with the parameters given above, Eqs. (17a) and (17b) can be written as the quasi-Makakov system

$$i \frac{\partial u_1}{\partial s} + \frac{1}{2} \frac{\partial^2 u_1}{\partial \sigma^2} + (|u_1|^2 + |u_2|^2) u_1 = R_1, \quad (24a)$$

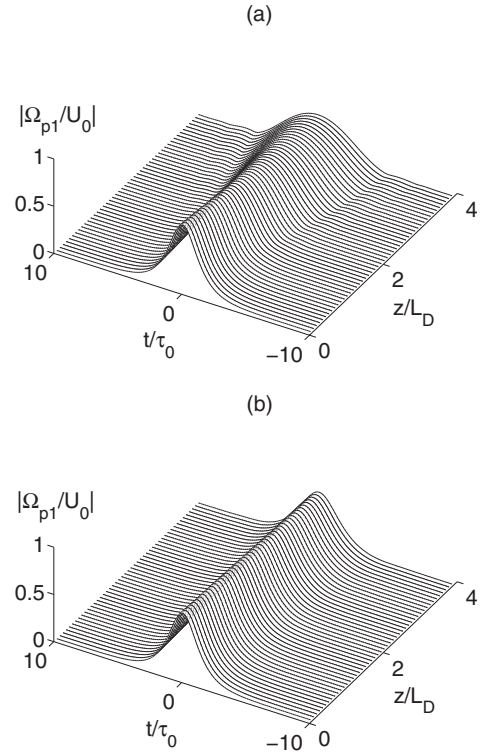


FIG. 4. $|\Omega_{p1}/U_0|$ as the function of the dimensionless time t/τ_0 and distance z/L_D . (a) Dispersion dominant case with $U_0 = 3.7 \times 10^6 \text{ s}^{-1}$. (b) The case of a balance between the dispersion and nonlinearity with $U_0 = 3.7 \times 10^7 \text{ s}^{-1}$.

$$i \frac{\partial u_2}{\partial s} + \frac{1}{2} \frac{\partial^2 u_2}{\partial \sigma^2} + (|u_2|^2 + |u_1|^2) u_2 = R_2, \quad (24b)$$

with $R_{1,2}(u_{1,2}) \approx -0.08iu_{1,2}$, describing a linear absorption effect. Because $R_{1,2}$ is a small quantity they can be taken as perturbations [36, 37] in the leading-order approximation. After neglecting $R_{1,2}$ the vector soliton solution of Eqs. (24a) and (24b) is given by [15]

$$u_1 = \cos \theta \text{sech}(\sigma) e^{is/2}, \quad (25)$$

$$u_2 = \sin \theta \text{sech}(\sigma) e^{is/2}, \quad (26)$$

with θ being a free real parameter. Note that since the injected probe field is linearly polarized, the two polarization components should have equal amplitude, i.e., $\theta = \pi/4$.

Shown in Fig. 4 is the evolution of the σ^- circular polarization component of the probe field versus dimensionless time t/τ_0 and distance z/L_D (the plots for the σ^+ circular polarization component are very similar, thus not shown). The figure is obtained by numerically integrating Eqs. (24a) and (24b) with complex coefficients by using a split-step Fourier transform method and the bright-bright soliton solution given above as an initial condition. To demonstrate the dispersion and nonlinear effects and their balance, we change the probe field amplitude U_0 while we keep other parameters the same as those given above. Figure 4(a) shows the result when the dispersion is dominant over the nonlinearity, i.e., $U_0 \tau_0 < \sqrt{|K_{22}/W_{22}|}$. We see that in this case the probe

field spreads significantly. However, if we choose $U_0\tau_0 = \sqrt{|K_{22}/W_{22}|}$, i.e., there is a balance between the dispersion and the nonlinearity, a shape-preserving propagation of vector optical soliton over a long distance to $4L_D$ is achieved, as clearly shown in Fig. 4(b).

The input power of the vector optical soliton can be calculated by Poynting's vector. It is easy to get the average flux of energy over carrier-wave period

$$\bar{P}_1 = \bar{P}_1^{\max} \operatorname{sech}^2[(t - z/V_{g1})/\tau_0], \quad (27)$$

$$\bar{P}_2 = \bar{P}_2^{\max} \operatorname{sech}^2[(t - z/V_{g2})/\tau_0]. \quad (28)$$

If choosing $|\mathbf{p}_{23}| \approx |\mathbf{p}_{43}| = 2.1 \times 10^{-27}$ cm C, R_\perp (the beam radius of the probe laser) = 0.01 cm, and the other parameters the same as those given above, one obtains the peak power of the vector soliton $\bar{P}_1^{\max} \approx \bar{P}_2^{\max} = 8.9 \times 10^{-4}$ mW. Thus to generate an ultraslow vector optical soliton in the present active EIT system only very low input power is needed. This is drastically different from the vector optical soliton generation schemes in fiber-based passive media [4–9, 11–14] where much higher input power of several tens of watts [8] or more is needed in order to bring out the nonlinear effect required for the soliton formation.

The property of the collision between two solitons is one of the most intriguing aspects in soliton dynamics. By using numerical simulations we have also investigated the feature of the collision between two ultraslow vector optical solitons in the present resonant system. Shown in Fig. 5 are the wave forms for several different two-soliton collisions in the σ^- circular polarization component of the probe field. A similar result for σ^+ circular polarization component is also obtained but not shown here. The initial condition in the simulation is chosen as $u_1(z=0) = (\sqrt{2}/2)\operatorname{sech}(\sigma - 3.0) \times \exp(-i\sigma) + \varrho(\sqrt{2}/2)\operatorname{sech}(\sigma + 3.0)\exp[i(\sigma + \theta_1)]$ and $u_2(z=0) = (\sqrt{2}/2)\operatorname{sech}(\sigma - 3.0)\exp(-i\sigma) + (\sqrt{2}/2)\operatorname{sech}(\sigma + 3.0) \times \exp[i(\sigma + \theta_2)]$, where $\sigma = t/\tau_0$, ϱ determines the initial relative amplitudes, and θ_1 and θ_2 denote the initial relative phases of the two solitons. As in conventional coupled NLS equations [34], our simulations also show that the collision property of the solitons depends on the relative amplitudes and the relative phases of the solitons.

Figure 5(a) shows the result with $\varrho = 1$ and $\theta_1 = \theta_2 = 0$. We see that in this case the interaction between the two solitons is attractive. The physical reason for the attraction is that the light intensity in the central region of the collision is increased by the overlap of the two solitons due to attractive interaction, which leads to an increase of the refractive index and hence attracts more light to the central region. Because of the particle property the solitons pass through each other and then propagate stably. However, a small attenuation occurs due to the absorption nature of the system.

In Fig. 5(b) we show the collision between the two solitons for $\varrho = 1$ and $\theta_1 = \theta_2 = \pi$. Different from Fig. 5(a), in this case the interaction between the two solitons is repulsive. This is because the refractive index is lowered when the two solitons overlap each other in the central region of the collision.

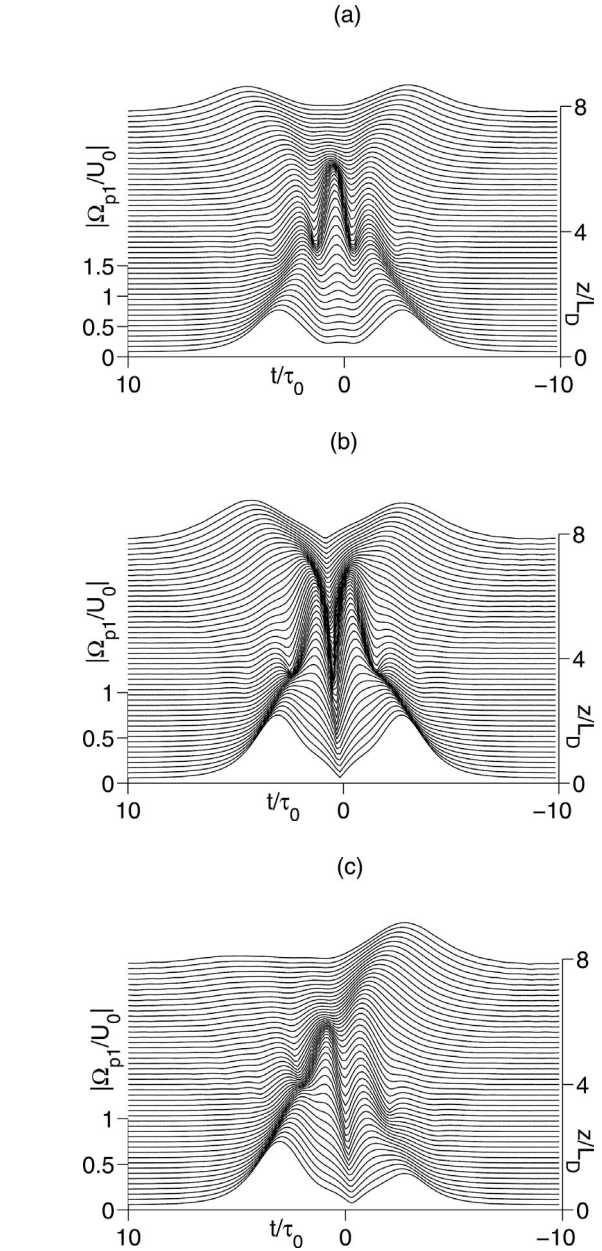


FIG. 5. The wave form of $|\Omega_{p1}/U_0|$ for several different two-soliton collisions. (a) $\varrho = 1$ and $\theta_1 = \theta_2 = 0$, (b) $\varrho = 1$ and $\theta_1 = \theta_2 = \pi$, (c) $\varrho = 0.5$, $\theta_1 = \pi/2$, and $\theta_2 = 0$.

tion. A small phase (position) shift can be observed during the collision.

Shown in Fig. 5(c) is the two-soliton collision for $\varrho = 0.5$, $\theta_1 = \pi/2$, and $\theta_2 = 0$. We find that in this case one soliton is completely absorbed while the other one undergoes no apparent deformation. This interesting inelastic colliding phenomenon of solitons in a two-component system has been also reported in Ref. [35], where the authors demonstrated that exact two-soliton solutions of the Manakov equations display a similar behavior. The collision property of solitons described above may have promising applications for all-optical information processing and engineering (e.g., for the design of soliton switching, etc.).

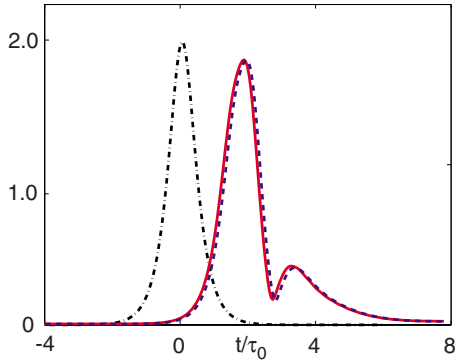


FIG. 6. (Color online) The bright-bright vector soliton evolution obtained by integrating directly from Eqs. (3a)–(3d), (5a), and (5b) without any approximation. The solid line (dashed line) is the result for $|\Omega_{p1}/U_0|$ ($|\Omega_{p2}/U_0|$) after propagating to the distance is $z = 1.2$ cm. The dotted-dashed line is the initial condition used in the simulation.

V. FURTHER DISCUSSION AND CONCLUSION

To make a further confirmation on the ultraslow vector soliton solutions obtained above and check their stability, we have made additional numerical simulations starting directly from Eqs. (3a)–(3d), (5a), and (5b) without using any approximation. Figure 6 provides the simulation result by taking the soliton wave form $u_{1,2}(z=0) = 2 \operatorname{sech}(2\sqrt{2}t/\tau_0)$ as an initial condition (shown by the dotted-dashed line). We see that after propagating the distance $z = 1.2$ cm, the main part of both polarization components $|\Omega_{p1}/U_0|$ and $|\Omega_{p2}/U_0|$ remains a soliton (shown by the solid and the dashed line, respectively). However, a radiation appears on the tail of the soliton, which is contributed by the high-order dispersion and high-order nonlinear effects of the system that are not included in the analytical approach given above [38].

In conclusion, we have proposed a scheme to produce temporal vector optical solitons in a lifetime broadened five-level atomic system via electromagnetically induced transparency. We have shown that, different from the optical solitons obtained in passive media such as optical fibers, the vector optical solitons in our active resonant system can be generated under very low light intensity and they have ultraslow propagating velocity. We have demonstrated both analytically and numerically that by using the present scheme it is easy to realize temporal Manakov vector optical solitons by actively manipulating the dispersion and nonlinear effects of the system. Due to their robust propagation nature, the ultraslow vector optical solitons suggested in this present work may have potential application in optical information processing and engineering under a weak-light level.

ACKNOWLEDGMENTS

This work was supported by the Key Development Program for Basic Research of China under Grant Nos. 2005CB724508 and 2006CB921104, by the NSF of China under Grant Nos. 10434060, 90403008, and 10674060, and by the Program for Changjiang Scholars and Innovative Research Team of Chinese Ministry of Education.

APPENDIX

1. Expressions of $M^{(l)}$, $N^{(l)}$, $P^{(l)}$, $Q^{(l)}$, $R^{(l)}$, and $T^{(l)}$

The explicit expressions of terms on the right-hand side of Eqs. (8a)–(8d), (9a), and (9b) are given by

$$M^{(1)} = N^{(1)} = P^{(1)} = Q^{(1)} = R^{(1)} = T^{(1)} = 0, \quad (\text{A1a})$$

$$M^{(2)} = -\frac{\partial}{\partial t_1} A_1^{(1)}, \quad (\text{A1b})$$

$$M^{(3)} = -\frac{\partial}{\partial t_1} A_1^{(2)}, \quad (\text{A1c})$$

$$N^{(2)} = -\frac{\partial}{\partial t_1} A_2^{(1)}, \quad (\text{A1d})$$

$$N^{(3)} = -\frac{\partial}{\partial t_1} A_2^{(2)} - i\Omega_{p1}^{(1)} A_3^{*(2)}, \quad (\text{A1e})$$

$$P^{(2)} = -\frac{\partial}{\partial t_1} A_4^{(1)}, \quad (\text{A1f})$$

$$P^{(3)} = -\frac{\partial}{\partial t_1} A_4^{(2)} - i\Omega_{p2}^{(1)} A_3^{*(2)}, \quad (\text{A1g})$$

$$Q^{(2)} = -\frac{\partial}{\partial t_1} A_5^{(1)}, \quad (\text{A1h})$$

$$Q^{(3)} = -\frac{\partial}{\partial t_1} A_5^{(2)}, \quad (\text{A1i})$$

$$R^{(2)} = -i \left(\frac{\partial}{\partial z_1} + \frac{1}{c} \frac{\partial}{\partial t_1} \right) \Omega_{p1}^{(1)}, \quad (\text{A1j})$$

$$R^{(3)} = -i \left(\frac{\partial}{\partial z_1} + \frac{1}{c} \frac{\partial}{\partial t_1} \right) \Omega_{p1}^{(2)} - i \frac{\partial}{\partial z_2} \Omega_{p1}^{(1)} + \kappa_{32} A_2^{(1)} A_3^{*(2)}, \quad (\text{A1k})$$

$$T^{(2)} = -i \left(\frac{\partial}{\partial z_1} + \frac{1}{c} \frac{\partial}{\partial t_1} \right) \Omega_{p2}^{(1)}, \quad (\text{A1l})$$

$$T^{(3)} = -i \left(\frac{\partial}{\partial z_1} + \frac{1}{c} \frac{\partial}{\partial t_1} \right) \Omega_{p2}^{(2)} - i \frac{\partial}{\partial z_2} \Omega_{p2}^{(1)} + \kappa_{34} A_4^{(1)} A_3^{*(2)}. \quad (\text{A1m})$$

2. Expressions of $\hat{\mathcal{L}}_1$ and $S_1^{(l)}$ and $S_2^{(l)}$

The expressions of the operators $\hat{\mathcal{L}}_1$, $\hat{\mathcal{L}}_2$ and the quantities $S_1^{(l)}$ and $S_2^{(l)}$ in Eqs. (10a) and Eqs. (10b) are defined by

$$\begin{aligned}\hat{\mathcal{L}}_1 &= -i \left(\frac{\partial}{\partial z_0} + \frac{1}{c} \frac{\partial}{\partial t_0} \right) \left[|\Omega_{c1}|^2 + \left(\frac{\partial}{\partial t_0} + id_1 \right) \left(\frac{\partial}{\partial t_0} + id_2 \right) \right] - i\kappa_{32} \left(\frac{\partial}{\partial t_0} + id_1 \right), \\ \hat{\mathcal{L}}_2 &= -i \left(\frac{\partial}{\partial z_0} + \frac{1}{c} \frac{\partial}{\partial t_0} \right) \left[|\Omega_{c2}|^2 + \left(\frac{\partial}{\partial t_0} + id_4 \right) \left(\frac{\partial}{\partial t_0} + id_5 \right) \right] - i\kappa_{34} \left(\frac{\partial}{\partial t_0} + id_5 \right), \\ S_1^{(l)} &= \kappa_{32} \left[i\Omega_{c1} M^{(l)} - \left(\frac{\partial}{\partial t_0} + id_1 \right) N^{(l)} \right] - \left[|\Omega_{c1}|^2 + \left(\frac{\partial}{\partial t_0} + id_1 \right) \left(\frac{\partial}{\partial t_0} + id_2 \right) \right] R^{(l)}, \\ S_2^{(l)} &= \kappa_{34} \left[i\Omega_{c2} Q^{(l)} - \left(\frac{\partial}{\partial t_0} + id_5 \right) P^{(l)} \right] - \left[|\Omega_{c2}|^2 + \left(\frac{\partial}{\partial t_0} + id_4 \right) \left(\frac{\partial}{\partial t_0} + id_5 \right) \right] T^{(l)}.\end{aligned}$$

-
- [1] C. R. Menyuk, *Opt. Lett.* **12**, 614 (1987).
[2] D. N. Christodoulides and R. I. Joseph, *Opt. Lett.* **13**, 53 (1988).
[3] M. V. Tratnik and J. E. Sipe, *Phys. Rev. A* **38**, 2011 (1988).
[4] M. N. Islam, C. D. Poole, and J. P. Gordon, *Opt. Lett.* **14**, 1011 (1989).
[5] Y. Barad and Y. Silberberg, *Phys. Rev. Lett.* **78**, 3290 (1997).
[6] S. T. Cundiff, B. C. Collings, N. N. Akhmediev, J. M. Soto-Crespo, K. Bergman, and W. H. Knox, *Phys. Rev. Lett.* **82**, 3988 (1999).
[7] A. E. Korolev, V. N. Nazarov, D. A. Nolan, and C. M. Truesdale, *Opt. Lett.* **30**, 132 (2005).
[8] D. Rand, I. Glesk, C.-S. Brès, D. A. Nolan, X. Chen, J. Koh, J. W. Fleischer, K. Steiglitz, and P. R. Prucnal, *Phys. Rev. Lett.* **98**, 053902 (2007).
[9] M. Segev, G. C. Valley, B. Crosignani, P. DiPorto, and A. Yariv, *Phys. Rev. Lett.* **73**, 3211 (1994).
[10] Z. Chen, M. Segev, T. H. Coskun, and D. N. Christodoulides, *Opt. Lett.* **21**, 1436 (1996).
[11] J. U. Kang, G. I. Stegeman, J. S. Aitchison, and N. Akhmediev, *Phys. Rev. Lett.* **76**, 3699 (1996).
[12] C. Anastassiou, J. W. Fleischer, T. Carmon, M. Segev, and K. Steiglitz, *Opt. Lett.* **26**, 1498 (2001).
[13] M. Delquè, T. Sylvestre, H. Maillotte, C. Cambournac, P. Kockaert, and M. Haelterman, *Opt. Lett.* **30**, 3383 (2005).
[14] M. N. Islam, *Ultrafast Fiber Switching Devices and Systems* (Cambridge University Press, Cambridge, 1992).
[15] S. V. Manakov, *Sov. Phys. JETP* **38**, 248 (1974).
[16] K. Steiglitz, *Phys. Rev. E* **63**, 016608 (2000).
[17] M. D. Lukin, P. R. Hemmer, and M. O. Scully, *Adv. At., Mol., Opt. Phys.* **42**, 386 (2000).
[18] M. Fleischhauer, A. Imamoglu, and J. P. Marangos, *Rev. Mod. Phys.* **77**, 633 (2005).
[19] L. V. Hau, S. E. Harris, Z. Dutton, and C. H. Behroozi, *Nature (London)* **397**, 594 (1999).
[20] M. M. Kash, V. A. Sautenkov, A. S. Zibrov, L. Hollberg, G. R. Welch, M. D. Lukin, Yu Rostovtsev, E. S. Fry, and M. O. Scully, *Phys. Rev. Lett.* **82**, 5229 (1999).
[21] H. Schmidt and A. Imamoglu, *Opt. Lett.* **21**, 1936 (1996).
[22] H. Kang and Y. Zhu, *Phys. Rev. Lett.* **91**, 093601 (2003).
[23] C. Ottaviani, D. Vitali, M. Artoni, F. Cataliotti, and P. Tombesi, *Phys. Rev. Lett.* **90**, 197902 (2003).
[24] D. Petrosyan, *J. Opt. B: Quantum Semiclassical Opt.* **7**, S141 (2005).
[25] Y. Wu and L. Deng, *Phys. Rev. Lett.* **93**, 143904 (2004); *Opt. Lett.* **29**, 2064 (2004).
[26] G. Huang, L. Deng, and M. G. Payne, *Phys. Rev. E* **72**, 016617 (2005).
[27] L. Deng, M. G. Payne, G. Huang, and E. W. Hagley, *Phys. Rev. E* **72**, 055601(R) (2005).
[28] G. Huang, K. Jiang, M. G. Payne, and L. Deng, *Phys. Rev. E* **73**, 056606 (2006).
[29] C. Hang, G. Huang, and L. Deng, *Phys. Rev. E* **73**, 036607 (2006).
[30] T. Hong, *Phys. Rev. Lett.* **90**, 183901 (2003).
[31] H. Michinel, M. J. Paz-Alonso, and V. M. Pérez-García, *Phys. Rev. Lett.* **96**, 023903 (2006).
[32] C. Hang, G. Huang, and L. Deng, *Phys. Rev. E* **74**, 046601 (2006).
[33] I. Friedler, G. Kurizki, O. Cohen, and M. Segev, *Opt. Lett.* **30**, 3374 (2005).
[34] A. Hasegawa and Y. Kodama, *Solitons in Optical Communications* (Clarendon, Oxford, 1995).
[35] R. Radhakrishnan, M. Lakshmanan, and J. Hietarinta, *Phys. Rev. E* **56**, 2213 (1997).
[36] T. I. Lakoba and D. J. Kaup, *Phys. Rev. E* **56**, 6147 (1997).
[37] J. Yang, *Phys. Rev. E* **59**, 2393 (1999).
[38] By using the method of multiple scales, one can further solve the fourth-order approximation of Eqs. (10a)–(10f). Then Eqs. (17a) and (17b) will be modified to have some additional terms contributed by high-order dispersion and high-order nonlinearities. The effect of these additional terms can be studied analytically by the perturbation theory of solitons [36,37].